PARP-3 localizes preferentially to the daughter centriole and interferes with the G1/S cell cycle progression

Angélique Augustin[1,*], Catherine Spenlehauer[1,*], Hélène Dumond[1], Josiane Ménissier-de Murcia[1], Matthieu Piel[2], Anne-Catherine Schmit[3], Françoise Apiou[4], Jean-Luc Vonesch[5], Michael Kock[6], Michel Bornens[2] and Gilbert de Murcia[1,‡]

[1]Unité 9003 du CNRS, Ecole Supérieure de Biotechnologie de Strasbourg, Boulevard Sébastien Brant, 67400 Illkirch, France
[2]Institut Curie, Section Recherche UMR 144 du CNRS, 26 Rue d'Ulm, F-75248 Paris, France
[3]Institut de Biologie Moléculaire des Plantes, CNRS, 12 rue du General Zimmer, 67084, Strasbourg, France
[4]Institut Curie, Section Recherche UMR 147 du CNRS, 26 Rue d'Ulm, F-75248 Paris, France
[5]Institut de Génétique et de Biologie Moléculaire et Cellulaire, CNRS/INSERM/ULP, Collège de France, BP 163, 67400 Illkirch, France
[6]Pharmaceuticals Research, BASF AG, D-67056 Ludwigshafen, Germany

*Both authors contributed equally to this work
‡Author for correspondence (e-mail: demurcia@esbs.u-strasbg.fr)

Accepted 2 January 2003
Journal of Cell Science 116, 1551-1562 © 2003 The Company of Biologists Ltd
doi:10.1242/jcs.00341

Summary

A novel member of the poly(ADP-ribose) polymerase (PARP) family, hPARP-3, is identified here as a core component of the centrosome. hPARP-3 is preferentially localized to the daughter centriole throughout the cell cycle. The N-terminal domain (54 amino acids) of hPARP-3 is responsible for its centrosomal localization. Full-length hPAPR-3 (540 amino acids, with an apparent mass of 67 kDa) synthesizes ADP-ribose polymers during its automodification. Overexpression of hPARP-3 or its N-terminal domain does not influence centrosomal duplication or amplification but interferes with the G1/S cell cycle progression. PARP-1 also resides for part of the cell cycle in the centrosome and interacts with hPARP-3. The presence of both PARP-1 and PARP-3 at the centrosome may link the DNA damage surveillance network to the mitotic fidelity checkpoint.

Key words: Centrosome, NAD^+ metabolism, DNA damage, G1/S cell cycle control, Midbody

Introduction

Poly(ADP-ribosyl)ation is an immediate post-translational modification of nuclear proteins induced by DNA damaging agents. At a site of DNA breakage, the enzymes poly(ADP-ribose) polymerase-1 (PARP-1, 113 kDa) and PARP-2 (62 kDa) catalyze the transfer of the ADP-ribose moiety from the respiratory co-enzyme NAD^+ to a limited number of acceptor proteins involved in chromatin architecture (histones H1, H2B, HMG proteins, lamin B and nucleolar proteins such as B23) and in DNA metabolism (DNA replication factors and topoisomerases including PARP-1) (D'Amours et al., 1999; de Murcia and Ménissier de Murcia, 1994; de Murcia and Shall, 2000). Poly(ADP-ribosyl)ation of these proteins establishes de facto a molecular link between DNA damage and chromatin modification and appears as an obligatory step in a detection/signaling pathway leading ultimately to the resolution of strand interruptions (Shall and de Murcia, 2000).

A superfamily of PARP-domain-containing proteins has recently emerged (Amé et al., 1999; Jacobson and Jacobson, 1999; Smith, 2001). From this family, PARP-1 and PARP-2 were until now the only characterized enzymes whose activity has been shown to be stimulated by DNA strand breaks (Amé et al., 1999; Schreiber et al., 2002). Acting as survival factors in mammalian cells under genotoxic stress, they are localized in the nucleus and possibly function as homo and/or heterodimers. Murine fibroblasts carrying a targeted disruption of either the *mPARP-1* or *mPARP-2* gene are defective in base excision repair (BER), indicating that PARP-1 and PARP-2 can reciprocally, but partially, compensate for the absence of each other (Schreiber et al., 2002).

VPARP (vault-PARP, PARP-4) was characterized through its interaction with the MVP (major vault protein) in yeast in a two-hybrid screen. Vault particles are large ribonucleoprotein complexes found in the cytoplasm of mammalian cells (Kickhoefer et al., 1999), which may have a transport function. VPARP poly(ADP-ribosyl)ates MVP in purified vaults, but the consequences of this modification on vaults properties remain elusive. Tankyrase-1 (PARP-5a) was initially identified through its interaction with the telomeric protein TRF1, a negative regulator of telomere length (Smith et al., 1998b). In vitro poly(ADP-ribosyl)ation by tankyrase-1 inhibits TRF1 binding to telomeric DNA, suggesting a role for tankyrase-1 in telomere function (Smith and de Lange, 2000). Overexpression of tankyrase-1 has recently been found to release TRF1 from telomeres, thus inducing their elongation (Smith and de Lange, 2000). Tankyrase-2 (PARP-5b) appears to interact with many partners at discrete subcellular locations, including the Golgi complex (Chi and Lodish, 2000) and endosomes (Lyons et al.,

2001). It also displays telomeric functions while interacting with tankyrase-1 (Cook et al., 2002). During mitosis VPARP and tankyrase-1 are located at the mitotic spindle (Kickhoefer et al., 1999) and in the pericentriolar region, respectively (Smith and de Lange, 1999).

A sequence encoding a 60 kDa protein with homology to PARP-1 and 2, called PARP-3, was previously discovered in an EST library screening using the catalytic domain sequence of hPARP-1 (Johansson, 1999). Using the same approach, we cloned a different human cDNA encoding a version of PARP-3 that was seven amino acids longer. Here we report that recombinant hPARP-3 is endowed with PARP activity in vitro. During the entire cell cycle, hPARP-3 is localized to the centrosome, the microtubule organising centre of animal cells, and resides preferentially in the daughter centriole. Given the potential role of centrosomes in cell cycle regulation, we tested whether hPARP-3 participates in the regulation of cell cycle checkpoints. Our results argue that hPARP-3 negatively influences the G1/S cell cycle progression without interfering with centrosome duplication. Moreover, we found that hPARP-3 interacts with hPARP-1, which was previously shown to be present at the centrosome as well (Kanai et al., 2000).

Materials and Methods

EST searches and isolation of cDNA clones

A human PARP-3 EST (#1889095) was identified in the LIFESEQ™ database of Incyte Pharmaceuticals using the human PARP-1 catalytic domain sequence for a database search. This EST was used to screen a human frontal cortex cDNA library cloned in UNI ZAP XR (Stratagene). The selected clone used in this study contained an insert of 2108 bp starting 94 nucleotides upstream of the ATG codon and covering the complete 1599 bp open reading frame encoding hPARP-3.

Fluorescence in situ hybridization (FISH) analysis

Human chromosomes were prepared from human peripheral blood lymphocyte cultures after BrdU incorporation during the last 7 hours before harvesting. Mouse chromosomes were prepared from normal mouse fibroblast cultures without BrdU incorporation. The full-length cDNA sequence encoding the *hPARP-3* gene and a 2.8 kb mouse *PARP-3* genomic clone (to be described elsewhere) were labelled by nick-translation with biotin-11-dUTP. 20 ng/μl hPARP-3 probe was hybridized to human chromosomes in hybridization buffer; the mouse PARP-3 probe was hybridized to mouse chromosomes at a concentration of 15 ng/μl, as previously described (Apiou et al., 1996). Detection of hybridization was performed using a goat anti-biotin antibody (Vector Laboratories, Peterborough, UK) and a rabbit anti-goat fluorescein isothiocyanate-conjugated antibody (P.A.R.I.S., Compiègne, France). Direct banding of 5-BrdU-substituted chromosomes stained with propidium iodide was obtained by incubation in an alkaline solution of p-phenylenediamine (PPD11) (Lemieux et al., 1992). Mouse chromosomes were stained with DAPI and identified by computer-generated reverse-DAPI banding. Metaphases were observed under a fluorescent microscope (DMRB, Leica, Germany). Images were captured using a cooled Photometrics CCD camera and Quips-smart capture software (Vysis).

Overproduction and purification of h PARP-3

hPARP-3 cDNA was cloned into the baculovirus transfer vector pFASTBAC1 (Life Technologies, Invitrogen, Cergy Pontoise, France). Sf9 cell propagation and protein production was performed according to Miranda et al. (Miranda et al., 1997). Purification of hPARP-3 was performed by affinity chromatography on Affigel-3-Aminobenzamide as previously described (Amé et al., 1999; Giner et al., 1992).

Plasmids

cDNA encoding hPARP-3 or its N-terminal domain (54 amino-acids) were cloned either into the eukaryotic expression vectors pBC (Chatton et al., 1995) in frame with GST, giving raise to pBC hPARP-3 and pBC N-ter hPARP-3, or into the pEGFP vector (Clontech), giving raise to pEGFP-hPARP-3 and pEGFP N-ter hPARP-3.

Poly(ADP-ribosyl)ation assay, western blot, south-western blot and GST pulldown

900 ng of purified hPARP-3 were incubated in 20 μl of buffer containing 100 mM Tris-HCl, pH 8.0, 10 μM NAD^+ and 10 μCi [^{32}P] NAD^+ (3 Ci/mmoles). After 15 minutes of incubation at 25°C, the reaction was stopped by dilution in the Laemmli buffer. Samples were analyzed on a 10% SDS-PAGE and blotted as described previously (Mazen et al., 1989) and autoradiographed on Kodak BiMax MS film. South-western blotting using [^{32}P]-labelled nick-translated activated DNA was performed as described previously (Mazen et al., 1989).

Two peptides matching the hPARP-3 N-terminal region (amino-acid 25-37 and 8-22) were used to elicit hPARP-3 polyclonal antibodies in rabbits (Ab 1650) and in mice (TJ56), respectively. Potential partners of hPARP-3 were isolated using the GST-pulldown technique described previously (Masson et al., 1998).

Cell culture and cell cycle analysis

Mammalian cell cultures were maintained at 37°C in 5% CO_2. The human lymphoblastic KE 37 cell line (Moudjou and Bornens, 1994) was grown in suspension in RPMI 1640 medium supplemented with 7% foetal calf serum (FCS) (GIBCO) and gentamicin. HeLa, CHO, 3T3 and HeLa HC1 cells stably expressing the fusion GFP-centrin (Piel et al., 2000) were cultured in DMEM containing 10% FCS and gentamicin. For cell cycle analysis, HeLa cells were transiently transfected by plasmids expressing GST alone or in fusion with hPARP-3 or N-ter hPARP-3. After 24 hours, cells were mock-treated or treated with 1 mM N-methyl N-nitrosourea (MNU) for 20 hours and trypsinized. Cell suspensions were washed twice in PBS containing 1% glucose, 1 mM EDTA and fixed with cold 70% ethanol in PBS for 2 hours. The fixed cells were then washed once with PBS, 1% glucose, 1 mM EDTA, once with PBS, 1% glucose, 1 mM EDTA, 0.1% Triton X100 and incubated for 45 minutes at room temperature with a monoclonal anti-GST antibody diluted 1:400. Cells were washed twice with PBS, 1% glucose, 1 mM EDTA, 0.1% Triton X100 and incubated with FITC-conjugated anti-mouse antiserum (Cappel) for 45 minutes at room temperature. After a last wash with PBS, 1% glucose, 1 mM EDTA, cells were incubated with 100 μg/ml RNaseA for 30 minutes at room temperature, stained with propidium iodide and analyzed with a FACScan flow cytometer using a gate on FITC-positive cells.

Isolation of centrosomes

Purified centrosomes were isolated from KE 37 cells according to the method described by Moudjou and Bornens (Moudjou and Bornens, 1994). The centrosome fractions were analyzed by immunofluorescence as described previously (Bornens and Moudjou, 1999).

Indirect immunofluorescence

Cells (5×10^4) grown on coverslips were transfected or not with the plasmids expressing GST- or GFP-fusion proteins and subsequently untreated or treated with various DNA-damaging agents, using either

γ-irradiation (10 Grays, 1.0 Gy/minute delivered by a ^{60}Co source) or a treatment with 1 mM N-methyl-N-nitrosourea (MNU) for 30 minutes or 1 mM H_2O_2 for 10 minutes. Amplification of centrosomes was evaluated in CHO cells treated with 4 mM Hydroxyurea (HU) for 48 hours prior to processing for immunochemistry (Meraldi et al., 2002; Meraldi et al., 1999). Following fixation with 100% methanol for 5 minutes at –20°C, cells were washed three times with PBS supplemented with 0.1% Tween (v/v). Cells were incubated overnight at 4°C or for 2 hours at room temperature, with a primary antibody – the polyclonal antibody anti-hPARP-3 (1650) (1:100), a monoclonal IgG2a antibody anti-p34^{cdc2} (1:200, Sigma), a monoclonal IgG2b antibody anti-acetylated α-tubulin (1:1000, Sigma) or a monoclonal antibody anti-glutamylated tubulin (Gt 335) (1:2000) or a monoclonal antibody anti-hPARP-1 (F1-23, 1:100). After washing, cells were incubated for 2 hours at room temperature with the appropriate conjugated secondary antibody: a Texas-Red-conjugated anti-rabbit antiserum (1:400, Sigma), a sheep FITC-conjugated anti-mouse antiserum (1:400, Sigma) or an Alexa Fluor (568 or 488) goat-anti-mouse IgG (1:1000, Molecular Probes). DNA was counterstained with DAPI. Immunofluorescence microscopy was performed using a Zeiss Axioplan equipped with a DP50 chilled CCD camera (Olympus) and the capture software ViewFinder Lite (Olympus). Alternatively, observations were made with a confocal microscope equipped with an argon/krypton laser and suitable barrier filters (Leica TCS4D, Heidelberg, Germany).

Results

hPARP-3 is a new member of the PARP family

A human PARP-3 EST was isolated using the sequence encoding the human PARP-1 catalytic domain. The human PARP-3 cDNA sequence encodes a 540 amino acid protein that encompasses a 54 amino acid N-terminal domain and a catalytic domain of 489 amino acids that has 39% identity (61% similarity) with the human PARP-1 catalytic domain. The sequence of hPARP-3 can be aligned with the other members of the PARP family (Fig. 1A). All of them contain the PARP signature that characterizes the ADP-ribose donor site (NAD^+) and the essential residues forming the poly(ADP-ribose) acceptor site including a catalytic glutamate (E522). In the hPARP-3 sequence the acceptor site is much less conserved, although it constitutes a part of the sequence that has strongly conserved secondary structure (Fig. 1B).

Analysis of the 5′ end of the human *PARP-3* gene (accession number: GenBank AY126341) revealed the presence of two potential splicing acceptor (AS) sites, AS1 and AS2 (Fig. 1C), which give rise to two proteins differing by seven amino acids at the N-terminus. A sequence of hPARP-3 has been previously published by Johansson (Johansson, 1999) that lacks the first seven N-terminal amino acids. In order to assess the real occurrence of the longest version, we used a PCR strategy to detect the 5′ end of hPARP-3 reverse-transcribed mRNA from normal human lung tissue (Fig. 1D). Primers were designed to match the nucleotide sequence encoding the longest form of hPARP-3 (PCR1). Under high stringency PCR conditions, the sense primer can hybridize only when AS2 is selected. As a PCR control, we used a second sense primer (PCR2) that matches hPARP-3 mRNA downstream of the splicing site whatever the type of mRNA in the cell. As shown in Fig. 1D, the PCR2 control product was 141 bp, as expected, and a unique band of 162 bp was detected in PCR1, which is in good agreement with the presence of the longest *PARP-3* encoding mRNA. Therefore, we concluded that a human PARP-3, which is seven residues longer than the amino-acid sequence published by Johansson (Johansson, 1999), is expressed in human cells. Nevertheless we cannot exclude the possibility that both sequences are present in cells, depending upon physiological conditions.

The chromosomal localization of the *hPARP-3* gene was identified by using FISH on human chromosomes using a human cDNA PARP-3 probe. Consistent signals on chromosome 3 band 3p21.1 to 3p21.31 were identified (Fig. 1E) and on chromosome 9, band F1-F2 in mouse (Fig. 1F-G), which confirms that hPARP-3 is a novel member of the PARP family encoded by a specific gene. As it is already the case for the *PARP-1* and *PARP-2* genes, a synteny was noticed between the human and mouse chromosomal regions coding for *PARP-3* genes.

Full-length hPARP-3 was overexpressed in the baculovirus/Sf9 system and purified by affinity chromatography on Affigel-3AB (Giner et al., 1992), yielding a polypeptide with an apparent molecular mass of 67 kDa (Fig. 2A, lane b). We took advantage of the unique N-terminal domain of hPARP-3, which has no counterpart in PARP-1 and PARP-2 to generate two polyclonal antibodies 1650 and TJ56. As shown in Fig. 2B (lanes f to j), anti-PARP-3 antibody 1650 recognizes the recombinant hPARP-3 as well as hPARP-3 in HeLa cell extracts. As expected, these antibodies did not crossreact with either hPARP-1 or hPARP-2 (data not shown).

The ability of hPARP-3 to synthesize ADP-ribose polymers in an autopoly(ADP-ribosyl)ation reaction was examined in an in vitro PARP activity assay using [^{32}P] NAD^+ as a substrate; the optimal concentration of 10 μM NAD^+ was determined. As shown in Fig. 2A (lane d), PARP-3 automodification occurs and is specifically inhibited by the competitive inhibitor 3-Aminobenzamide (3-AB) (lane e). Interestingly, a slight increase in enzymatic activity (two-fold) was repeatedly observed in the presence of nicked DNA, in accord with the capacity of the N-terminal domain to bind DNA in a south-western assay (Fig. 2A, lane c). Altogether, these results clearly indicate that PARP-3 is a bona fide poly(ADP-ribose) polymerase.

hPARP-3 localizes preferentially to the daughter centriole throughout the cell cycle

To establish the subcellular localization of hPARP-3, exponentially growing HeLa cells were stained with the purified hPARP-3 antibody 1650. hPARP-3 localized to two closely spaced dots resembling centrosomes, usually located close to the nuclear envelope. As a control, we performed a double immunofluorescence experiment using the anti-hPARP-3 antibody 1650 and an antibody raised against p34^{cdc2}, as p34^{cdc2} has been previously shown to localize to centrosomes (Bailly et al., 1989; Pockwinse et al., 1997). As shown in Fig. 3A, the immunostaining of hPARP-3 was clearly associated with the centrosomal staining of p34^{cdc2}. To verify this observation, HeLa HC1 cells constitutively expressing the centrosomal protein centrin in fusion with GFP (Piel et al., 2000; White et al., 2000) were immunostained with the anti-hPARP-3 antibody 1650. The colocalization of hPARP-3 with GFP-centrin is clearly visible in Fig. 3B and confirms the association of PARP-3 with the centrosome. A similar result was obtained with the mouse polyclonal TJ56 antibody (data not shown). Staining of centrosomes was independent of the fixation method, as it was observed following procedures based

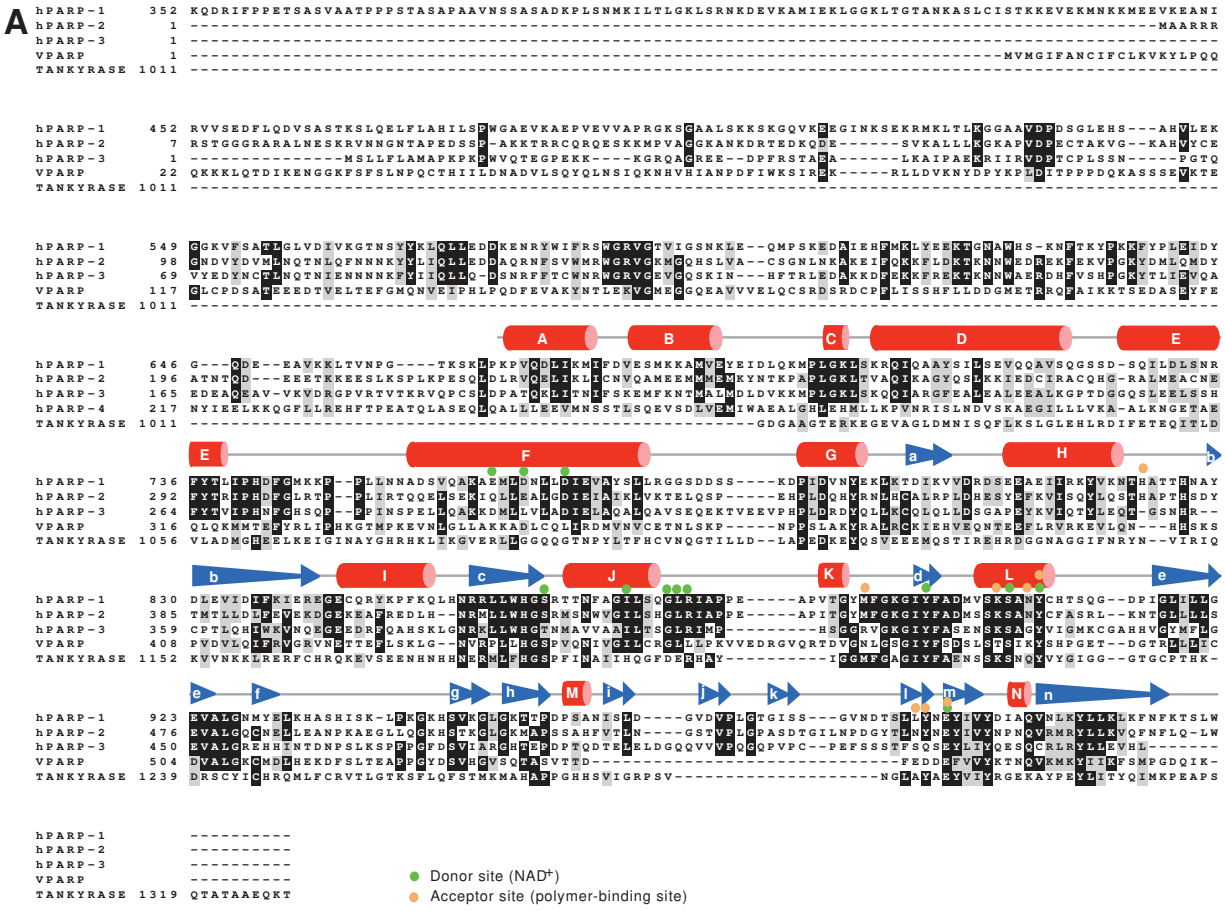
A
hPARP-1
hPARP-2
hPARP-3
VPARP
TANKYRASE
A
B
C
D
E
E
F
G
H
b
I
c
J
K
d
L
e
f
g
h
M
i
j
k
l
m
N
n
Donor site (NAD+)
Acceptor site (polymer-binding site)

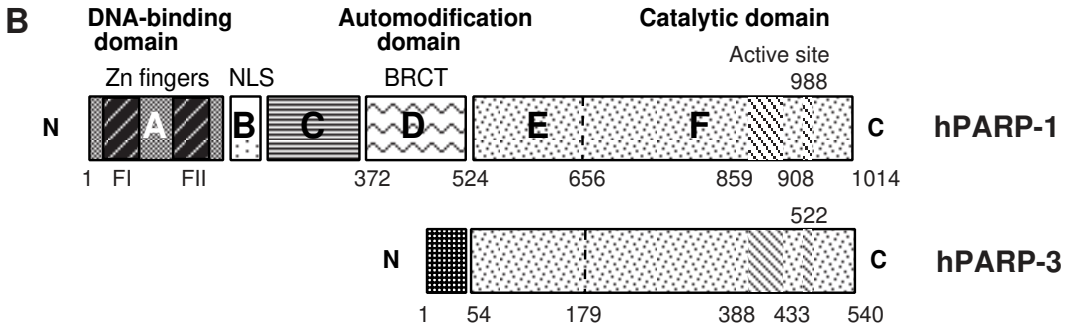
B
DNA-binding domain
Zn fingers
NLS
Automodification domain
BRCT
Catalytic domain
Active site
988
N
A
B
C
D
E
F
C
hPARP-1
1
FI
FII
372
524
656
859
908
1014
522
N
C
hPARP-3
1
54
179
388
433
540

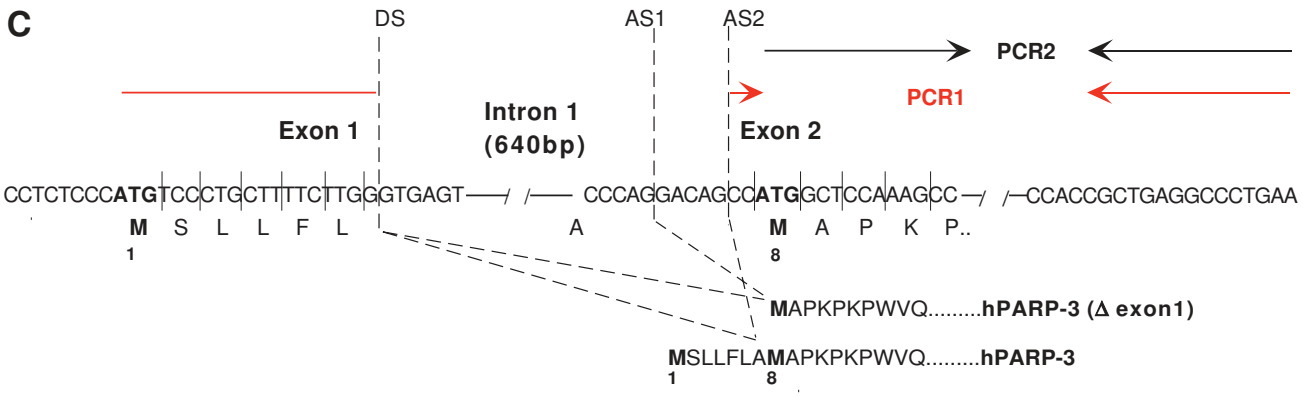
C
DS
AS1
AS2
PCR2
PCR1
Exon 1
Intron 1
(640bp)
Exon 2
CCTCTCCCATGTCCCTGCTTTCTTGGGTGAGT
CCCAGGACAGCCATGGCTCCAAAGCC
CCACCGCTGAGGCCCTGAA
M S L L F L
A
M A P K P..
1
8
MAPKPKPWVQ.....hPARP-3 (Δ exon1)
MSLLFLAMAPKPKPWVQ.....hPARP-3
1
8

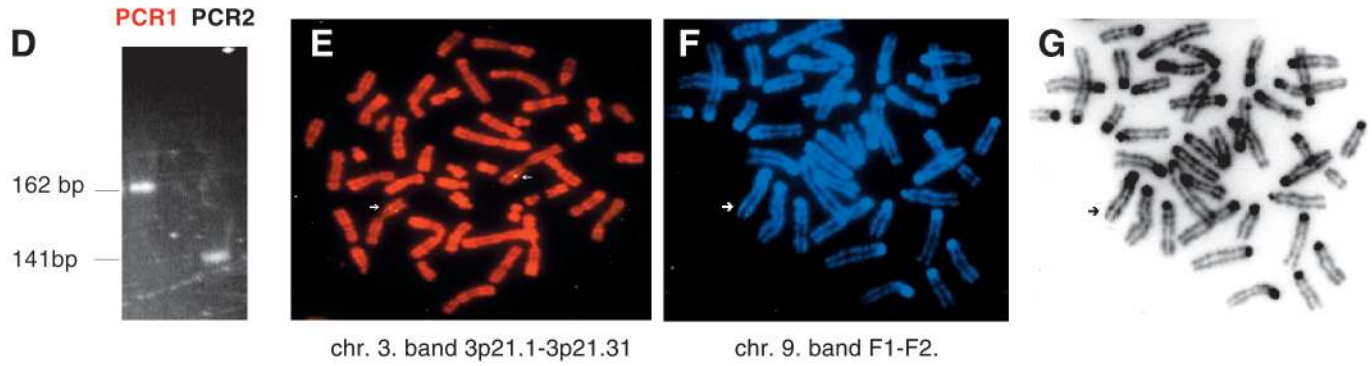

Fig. 1. (A) Sequence alignment of the five first members of the PARP family. Sequence alignment of amino acids 352 to 923 of human PARP-1 [hPARP-1, accession number P09874 (Cherney et al., 1987; Kurosaki et al., 1987; Uchida et al., 1987)], human PARP-2 [hPARP-2, AJ236912, (Ame et al., 1999)], human PARP-3 [hPARP-3, accession number NM_005485 (Johansson, 1999)], vault-particle-associated PARP [VPARP, accession number AF057160 (Kickhoefer et al., 1999)] and tankyrase [accession number AF082556 (Smith et al., 1998b)]. Cylinders and arrows schematically represent α helices and β-strands, respectively, as previously shown in the chicken PARP-1 structure (Ruf et al., 1996). (B) Schematic representation of the functional domains of hPARP-1 and hPARP-3. (C) Structure of the two possible versions of the human PARP-3 gene product by alternative splicing of the first exon. AS, acceptor site; DS, donor site. (D) PCR products loaded on 6% polyacrylamide gel. (E) Chromosomal mapping of *hPARP-3*: FISH of the *hPARP-3* gene on a human lymphocyte chromosome spread (arrows). Chromosomes are counterstained with propidium iodide. (F,G) Chromosomal mapping of mouse PARP-3: FISH of mPARP-3 on a mouse fibroblasts chromosome spread. Chromosomes are counterstained with DAPI. The sequence data of hPARP-3 is available from GenBank/EMBL/DDBJ under accession number AY126341.

on either aldehyde or organic solvent fixation. Finally, cell treatment with a microtubule-depolymerizing drug such as nocodazole or with a microtubule-stabilizing drug such as taxol did not displace the centrosomal signal emerging from the anti-PARP-3 antibodies (data not shown), demonstrating that the localization of hPARP-3 to the centrosome is independent of microtubule dynamics.

Strikingly, a preferential colocalization of hPARP-3 with one of the two centrioles was repeatedly noticed (Fig. 3C). The nature of the two centrioles can be distinguished by using immunocytochemistry in mouse 3T3 cells (Chang and Stearns, 2000; Lange and Gull, 1995). In G1 phase, the mother centriole of these cells grows a primary cilium, which is partially made of an acetylated form of α-tubulin. As shown in Fig. 3D, the signal corresponding to hPARP-3 antibodies cannot be superimposed on the signal from anti-acetylated α-tubulin antibodies, therefore suggesting that hPARP-3 colocalizes preferentially with the daughter centriole. A similar conclusion could be reached from colocalization experiments using HeLa HC1 cells, where the reproducible association of hPARP-3 with the 'smaller' (daughter) centriole was clearly visible (Fig. 3C).

We next examined the stage of the cell cycle that hPARP-3 associates with the centrosome. Following immunostaining of exponentially growing HeLa HC1 cells, hPARP-3 could unequivocally be identified at the centrosome in >90% of cells, independently of the antibody used. Moreover, confocal microscopy revealed a colocalization of hPARP-3, mostly with one of the two centrioles, most probably the daughter one, in G2 and throughout mitosis from early prophase to telophase (Fig. 3E). Taken together, these data demonstrate that hPARP-3 is a core component of the centrosome and is preferentially associated with the daughter centriole at all stages of the cell cycle.

Purified centrosomes are enriched in hPARP-3

To further substantiate the cellular distribution of hPARP-3,

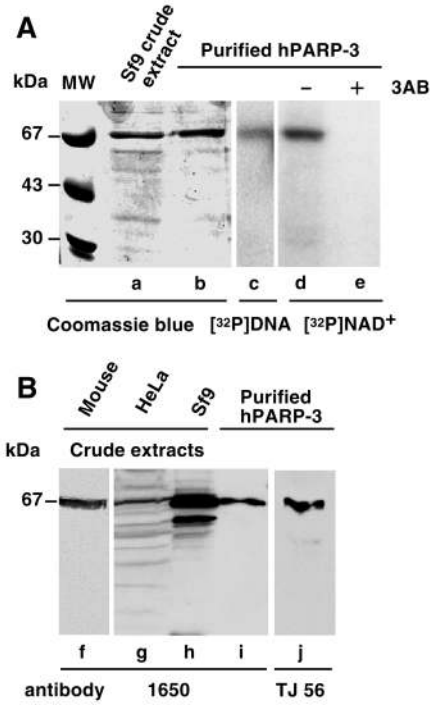

Fig. 2. (A) Purification and characterization of recombinant hPARP-3 overexpressed in the Sf9/baculovirus system. Crude extract from infected Sf9 cells (lane a); Purified recombinant hPARP-3 (lanes b-e); DNA-binding activity of hPARP-3 detected by south-western blotting (lane c); autopoly(ADP-ribosyl)ation of purified hPARP-3 incubated with [α-^{32}P] NAD^+ (lane d); inhibition of hPARP-3 autopoly(ADP-ribosyl)ation by 2 mM 3-Aminobenzamide (lane e). (B) Western blot detection of hPARP-3 in crude extracts from mouse lung (lane f), HeLa cells (lane g) or infected Sf9 cells (lane h) and purified recombinant hPARP-3 (lanes i,j) using two different anti hPARP-3 antibodies (see Materials and Methods).

centrosomes were isolated from KE 37 cells (Moudjou and Bornens, 1994) and examined by indirect immunofluorescence (Fig. 4A). Centrosomes were spun down on coverslips and co-stained with the anti-p34^{cdc2} antibody, to label centriole doublets, and with the purified polyclonal anti-PARP-3 antibody 1650. Again, a specific staining of one of the two centrioles was observed, in agreement with the above results obtained with whole cells.

The presence of hPARP-3 in the centrosome was also confirmed biochemically (Fig. 4B). Low-speed Triton X-100 soluble and insoluble fractions of unsynchronized KE 37 cell lysates were prepared as described previously (Tassin and Bornens, 1999) and submitted to western blot analysis together with centrosome sucrose gradient preparations (Moudjou and Bornens, 1994) and recombinant hPARP-3. Proteins were probed with the affinity-purified anti-hPARP-3 antibody 1650 (Fig. 4B). A band at 67 kDa is observed in enriched centrosomes, as well as in the Triton-insoluble fraction and to a lesser extent in the Triton-soluble fraction of KE 37 cells.

DNA damage does not affect hPARP-3 localization

Sato et al. have previously

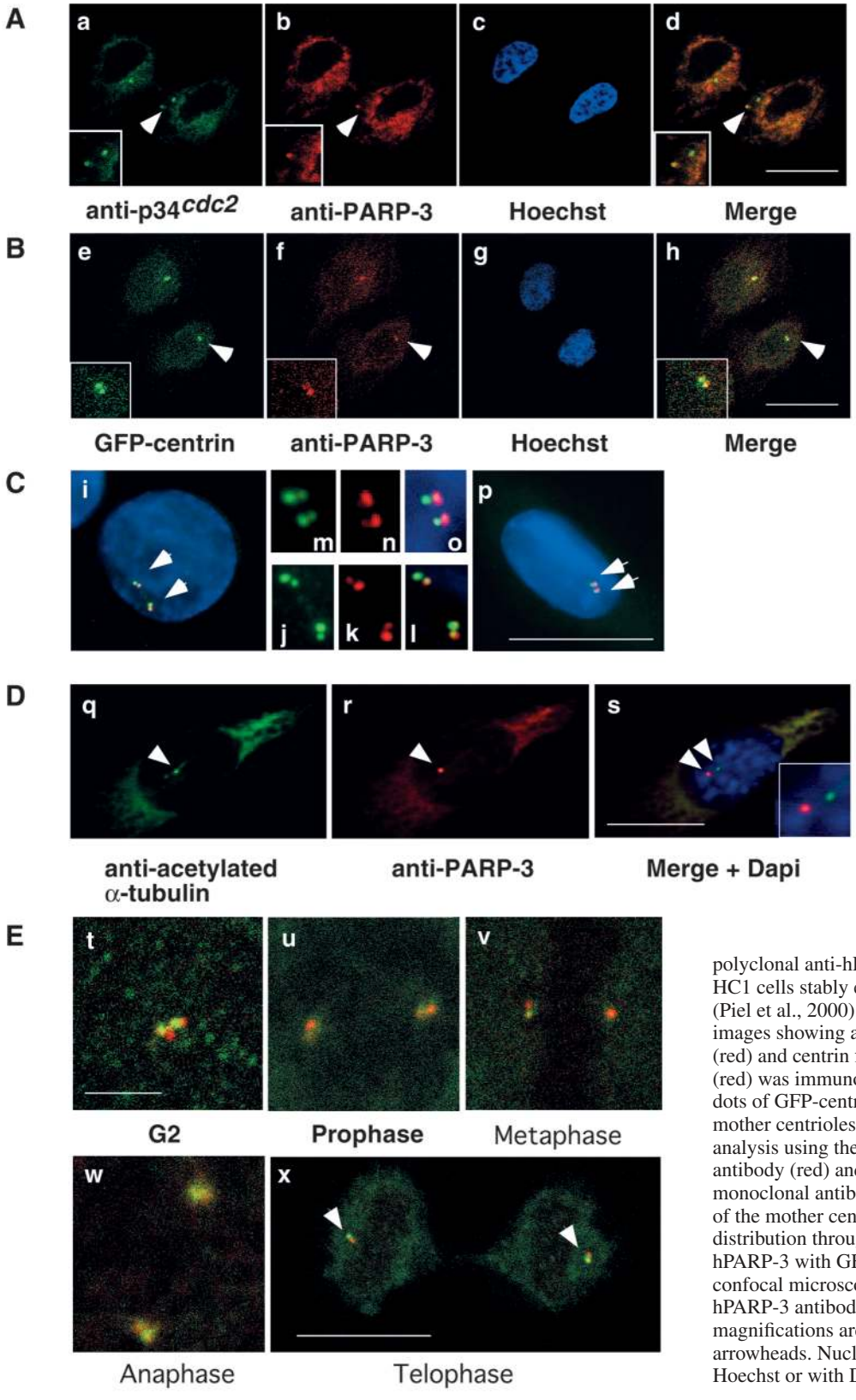

Fig. 3. hPARP-3 preferentially localizes to the daughter centriole throughout the cell cycle. (A) Confocal imaging of the subcellular distribution of hPARP-3 (red) at the centrosome marked with the anti-p34^{cdc2} antibody (green) in HeLa cells; d is a merge of a and b; (B) Colocalization of hPARP-3 immunostained with the polyclonal anti-hPARP-3 antibody 1650 (red) with HeLa HC1 cells stably expressing centrin (green) fused to GFP (Piel et al., 2000). h is a merge of e and f. (C) Merged images showing an asymmetric distribution of hPARP-3 (red) and centrin fused to GFP in S/G2 cells. hPARP-3 (red) was immunostained as in B. Strongly fluorescent dots of GFP-centrin (insets m and j) are attributed to the mother centrioles. (D) Immunofluorescence microscopy analysis using the 1650 polyclonal anti-hPARP-3 antibody (red) and the anti-acetylated α-tubulin monoclonal antibody (green) showing the primary cilium of the mother centriole. (E) hPARP-3 subcellular distribution throughout the cell cycle. Colocalization of hPARP-3 with GFP-centrin in HeLa HC1 cells by confocal microscopy analysis using the polyclonal anti-hPARP-3 antibody 1650 (red). For all pictures, the magnifications are details of the area surrounding the arrowheads. Nuclei in c, g, i, p and s are stained with Hoechst or with DAPI in S phase. Bars, 10 μm.

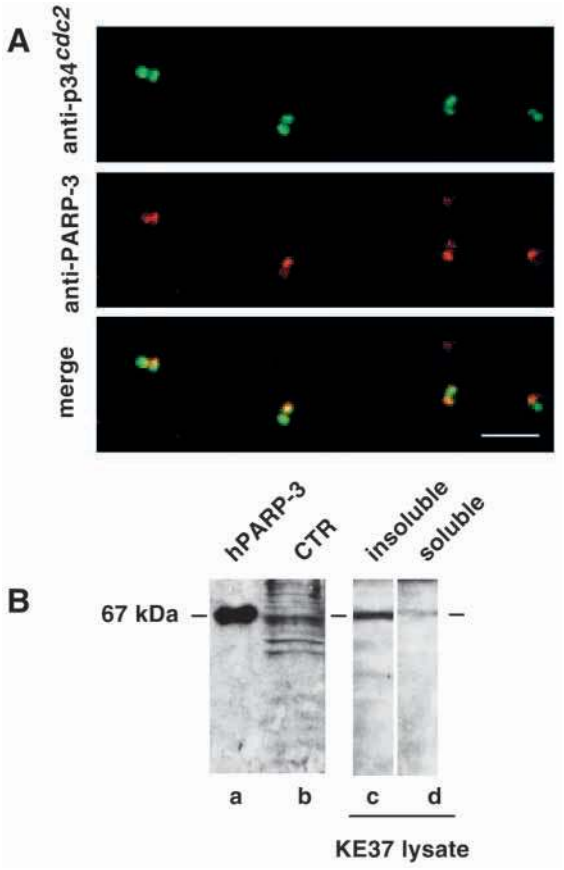

Fig. 4. hPARP-3 is detected in purified centrosomes. (A) Immunostaining of centrosome preparations from KE 37 cells. Immunolabelling was carried out using an anti-p34^{cdc2} antibody (green) and the polyclonal anti-hPARP-3 antibody 1650 (red). Bar, 2 μm. (B) Western blot of purified recombinant hPARP-3 (lane a), a sample of purified centrosomes (10^8) (lane b) and a KE 37 lysate containing a highly enriched centrosome preparation present in both the Triton-insoluble (lane c) and Triton-soluble fractions (lane d).

reported that γ-irradiation of U2-OS osteosarcoma cells or HeLa cells results in centrosome overduplication (Sato et al., 2000). Moreover, we and others have demonstrated that radiation-induced DNA strand-breaks activate PARP-1 and PARP-2 in the nucleus. We thus examined the hPARP-3 localization in HeLa HC1 cells exposed to various DNA-damaging agents including γ-radiation, N-methyl-N-nitrosourea (MNU) or H_2O_2 treatment. Asynchronous HeLa HC1 cells were irradiated at a single dose of 10 Gy or treated with 1 mM MNU or 1 mM H_2O_2; the centrosome number and hPARP-3 subcellular localization were subsequently determined by immunofluorescence at various time points following DNA damage (Fig. 5 and data not shown). Although the abnormal cells with more than two centrioles were less than 5% of the population in untreated cells, this population increased up to 70% by 120 hours post-irradiation or 72 hours post-MNU treatment as previously (Sato et al., 2000). Whatever the type of DNA injury, multipolar spindles (Fig. 5A-C) and coalescence of centrosomes (Fig. 5D-F) were frequently observed, as already described (Brinkley, 2001). However, co-staining of treated cells with the affinity-purified anti-hPARP-3 antibody and the anti-p34cdc2 antibody revealed that hPARP-3 was always present in the centrosome even under DNA damage conditions. Therefore, the localization of hPARP-3 is not affected by centrosome dynamics in response to DNA-damaging agents.

Overexpression of hPARP-3 or its N-terminal domain interferes with the cell cycle progression at the G1/S transition

Given the tight link between centrosome homeostasis and cell cycle regulation, we tested whether hPARP-3 participates in cell cycle regulation in mock or DNA-damage-exposed cells. We transiently expressed in HeLa cells the full-length hPARP-3 or its N-terminal domain as a glutathione S-transferase (GST)-fusion protein, and the cell cycle distribution of the GST-expressing cells was analyzed. As displayed in Fig. 6A, in untreated cells the expression of both hPARP-3 or its N-terminal domain caused an imbalance in normal cell cycle distribution characterized by an increase in the fraction of cells in G1/S compared to cells expressing GST alone.

DNA damage checkpoints arrest the cell cycle at the G2/M boundary to allow DNA repair, thus preventing progression of cells into mitosis. Following DNA base damage induced by a treatment with MNU, HeLa cells expressing only GST showed, as expected, a prominent

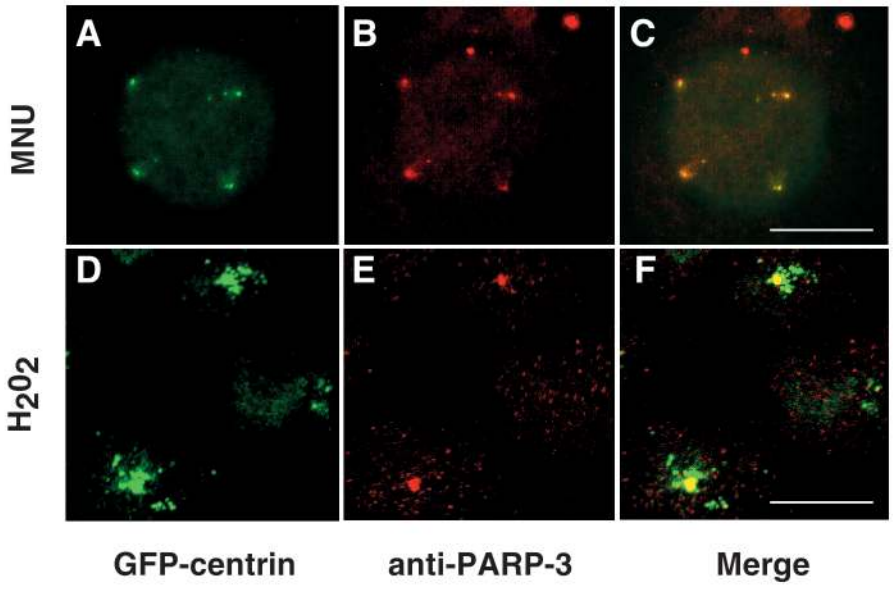

Fig. 5. DNA damage induces centrosome amplification but does not relocate hPARP-3. HeLa HC1 cells expressing GFP-centrin (green) were immunostained with an anti-hPARP-3 (red) antibody 120 hours after treatment with 1 mM MNU (A-C) or with 1 mM hydrogen peroxide (D-F). Examples of monopolar and multipolar spindles are shown. Bars, 10 μm.

accumulation at the G2/M boundary (39%). In contrast, the proportion of cells at the G2/M boundary was markedly decreased in cells expressing GST-N-ter hPARP-3 or GST-hPARP-3 (13% and 22% respectively); instead the GST fusion protein accumulated at the G1/S boundary. Together, these results imply that hPARP-3 acts at the G1/S cell cycle transition and that this function is carried out by its N-terminal domain but not by its catalytic domain.

To better correlate the biological function of hPARP-3 with its localization at the centrosome, we transiently expressed in HeLa cells the full-length hPARP-3 or its N-terminal domain as GFP fusions and analyzed their subcellular distribution using anti-γ-tubulin antibodies as centrosome markers. As shown in Fig. 6B, hPARP-3 (panel d-f), and more precisely its 54 amino-acid N-terminal domain (panel a-c), contains a motif responsible for centrosomal retention. This centrosomal localisation paralleled the G1/S cell cycle accumulation, as the exon-1-deleted version of the hPARP-3 N-terminal domain in fusion with GST did not target to the centrosome and did not

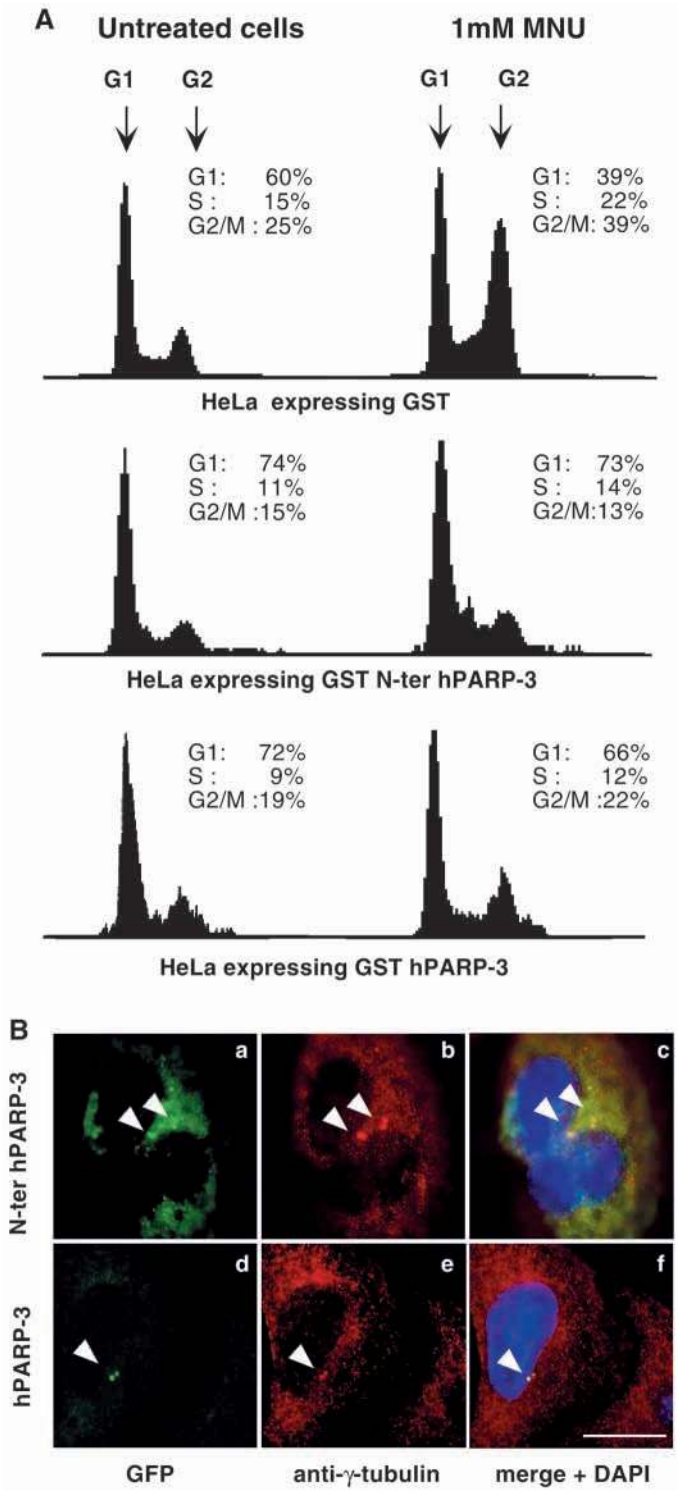

Fig. 6. (A) hPARP-3 or N-ter hPARP-3 overexpression leads to G1/S cell cycle arrest. FACS analysis on undamaged (left column) and MNU-treated (right column) HeLa cells expressed by GST, GST N-ter hPARP-3 or GST-hPARP-3. (B) hPARP-3 (d-f) or its N-terminal domain (a-c) target the GFP fusion protein to the centrosome, which is immunostained with an anti γ-tubulin antibody (red). Bar, 10 μm.

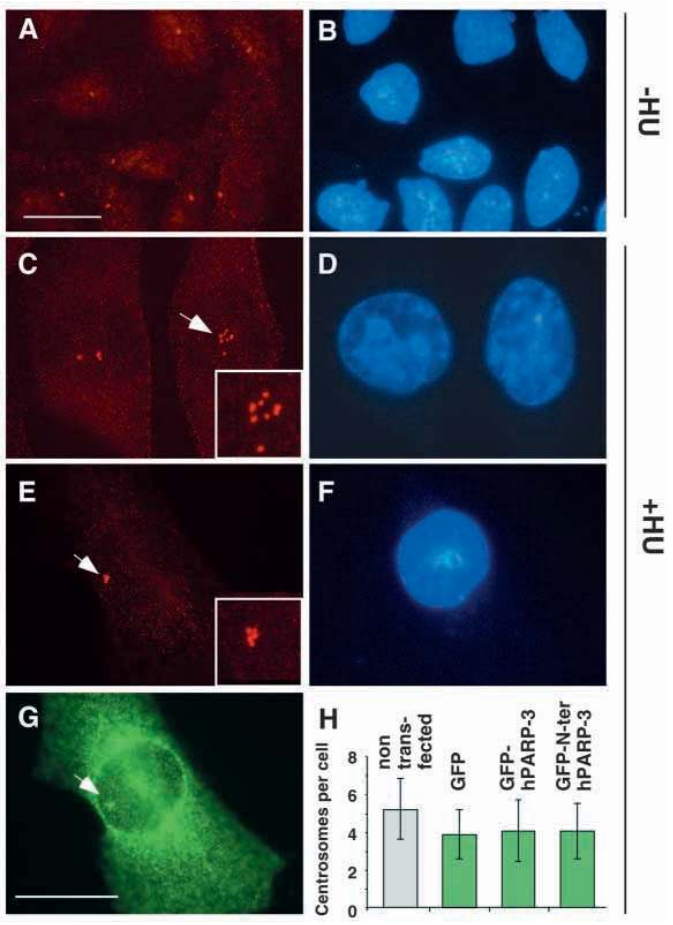

Fig. 7. hPARP-3 overexpression does not prevent centrosome amplification induced by hydroxyurea (HU) in CHO cells. Cells were transfected for 48 hours to express full-length or N-ter hPARP-3 as GFP-fusion proteins and cultured in the presence (C-F) or absence (A-B) of HU. Transfected cells were identified by fluorescence microscopy, and the number of centrosomes quantified using the antibody anti-glutamylated tubulin Gt335 (red). (C,D) Non-tranfected cells. (E-G) Transfected cells expressing GFP-hPARP-3. (H) Histogram showing the mean number of centrosomes±s.d. counted in non-transfected cells or in cells expressing GFP alone, GFP-hPARP-3 or GFP-N-ter hPARP-3 following HU treatment. The arrows point to centrosome amplification. Bars, 10 μm.

induce a G1/S accumulation when overexpressed in HeLa cells (data not shown).

hPARP-3 overexpression does not interfere with centrosome overduplication induced by hydroxyurea treatment

We considered the possibility that the G1/S block observed in cells expressing GST-N-ter hPARP-3 or GST-hPARP-3 is caused by an inhibition of centrosome duplication. To test this hypothesis, the GFP-hPARP-3 or GFP-N-ter hPARP-3 constructs were tested for their ability to interfere with centrosome duplication in an assay developed by Balczon et al. (Balczon et al., 1995). This assay is based on the observation that hydroxyurea (HU) treatment of CHO cells blocks DNA replication but allows multiple rounds of centrosome replication to occur. Following 40 hours of treatment, more than 50% of cells contain more than two centrosomes (Balczon et al., 1995; Matsumoto et al., 1999; Meraldi et al., 1999). As displayed in Fig. 7E-G, CHO cells expressing GFP-hPARP-3 were not affected by centrosome overamplification (Fig. 7C,D). Similar results were obtained with CHO cells expressing the GFP-N-ter hPARP-3.

To quantify the amplification of centrosomes, the number of spots obtained after anti-γ-tubulin staining were counted, and the mean values±s.d. for at least 50 cells were calculated and plotted on a histogram (Fig. 7H). For cells expressing GFP in fusion with hPARP-3 or its N-terminal domain, we detected, respectively, 4.3±1.6 (range 1 to 9) and 4.2±1.5 (range 2 to 7) centrosomes. This number is slightly decreased compared with non-transfected cells, which display 5.4±1.6 (range 2 to 10) centrosomes, but quite similar to the number (4.1±1.3, range 2 to 7) of centrosomes detected in cells expressing GFP alone. Overall, these results suggest that the G1/S cell cycle block mediated by hPARP-3 overexpression is not due to direct inhibition of centrosome duplication.

PARP-3 interacts with PARP-1 at the centrosome

Both the previously demonstrated localization of hPARP-1 to the centrosome (Kanai et al., 2000) and the ability of different PARPs to interact with each other (Sbodio et al., 2002; Schreiber et al., 2002) prompted us to investigate the possibility of a contact between hPARP-3 and hPARP-1. To this end, hPARP-3 or its N-terminal domain was transiently

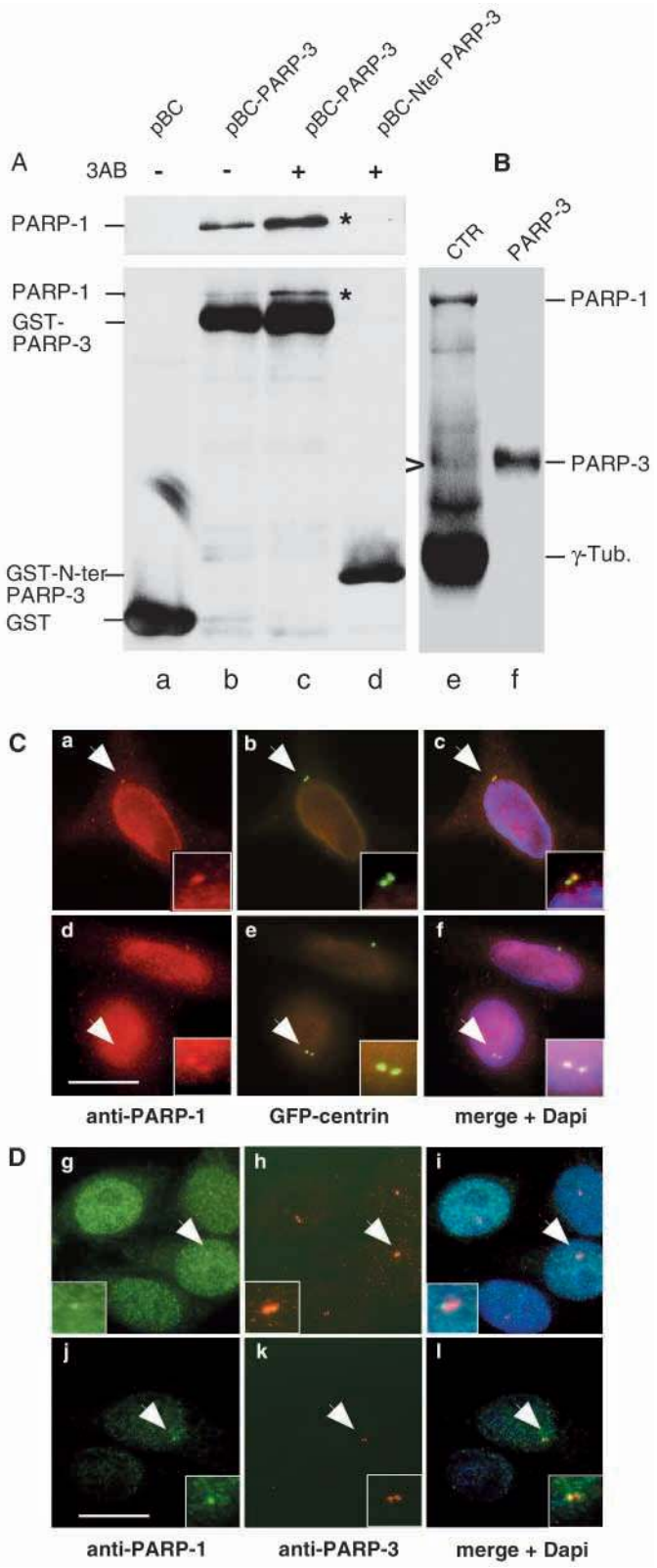

Fig. 8. hPARP-3 interacts with hPARP-1 at the centrosome. (A) Extracts from HeLa cells expressing either GST (lane a), GST-hPARP-3 (lanes b and c) or GST-N-ter hPARP-3 (lane d) were submitted to GST pull-down experiments, and the interacting proteins were analyzed by western blotting. When indicated, a treatment with 2 mM 3AB was applied for 2 hours before harvesting cell extracts. The blot was firstly probed with the mouse anti-hPARP-1 antibody (EGT69) (asterisks in upper panel) and subsequently with a polyclonal anti-GST antibody to reveal the proper expression of the fusion proteins (lower panel). (B) Sample of purified centrosomes (10^7) separated on SDS-PAGE and analyzed by western blotting using successively antibodies against hPARP-1, hPARP-3 and γ-tubulin (lane e); purified recombinant hPARP-3 (50 ng) (lane f). (C) Subcellular localization of hPARP-1 in GFP-centrin expressing HeLa HC1 cells. hPARP-1 was detected using a monoclonal antibody (F1-23) followed by the anti-mouse fluor Alexa 568 conjugate (red). (D) Both hPARP-1 and hPARP-3, immunostained with their respective specific antibodies, are detected at the centrosome in HeLa cells. For all pictures, the magnifications are details of the area surrounding the arrowheads. Bars, 10 μm.

overexpressed as a GST-fusion proteins in HeLa cells, and the interacting proteins were analyzed by western blotting. As shown in Fig. 8A, hPARP-1 was captured by the GST-hPARP-3 fusion protein but not by GST alone or GST fused to the N-terminal domain of hPARP-3. Moreover, the contact between hPARP-1 and hPARP-3 could be substantially enhanced when poly(ADP-ribose) synthesis was inhibited in the presence of the PARP inhibitor 3-aminobenzamide (Fig. 8A, compare lanes b and c), demonstrating an increased affinity of hPARP-1 and hPARP-3 for their respective unmodified form.

Proof of this interaction was further strengthened by the detection of both hPARP-1 and hPARP-3 in enriched fractions of purified centrosomes, which were characterized by the presence of γ-tubulin, a major component of centrosomes (Fig. 8B). Thus, the probability that the two PARPs interact is thought to be highest in this subcellular compartment. Indirect immunofluorescence experiments confirmed that hPARP-1 also resides in the centrosome. Indeed, hPARP-1 colocalizes with GFP-centrin in HeLa HC1 cells stably expressing this typically centrosomal protein (Fig. 8C). Despite the large nuclear staining of hPARP-1 and the close proximity of centrosomes to the nucleus, which makes it harder to affirm the centrosomal localization of hPARP-1, the colocalization of hPARP-1 and hPARP-3 could be performed using their respective antibodies (Fig. 8D). Taken together, these results indicate that hPARP-1 is present in both centrioles and interacts with hPARP-3, most probably at the daughter centriole. The enzymatic activity of both enzymes at the centrosome could be visualized in purified centrosome spreadings following incubation with NAD^+ and immunostaining with the anti-poly ADP-ribose antibody (data not shown). Finally, using PARP-1 knockout cell lines, we could demonstrate that the location of mPARP-3 at the centrosome was independent of the presence of mPARP-1 (data not shown).

Discussion

PARP-3 is a bona fide poly(ADP-ribose) polymerase

In this work, we have characterized a novel member of the PARP family, PARP-3. hPARP-3 catalyzes the synthesis of poly(ADP-ribose) in vitro and in purified centrosome preparations, presumably through an automodification mechanism. Like most of the other novel PARPs, with the exception of VPARP, the catalytic domain of hPARP-3 is located at its C-terminus. The N-terminal region, which is particularly short in the case of hPARP-3 (54 residues), apparently contains a targeting motif that is sufficient to localize the enzyme or the reporter protein GFP to the centrosome. No significant sequence homologous to this part has yet been found in the data banks. Moreover, the presence of basic residues in its N-terminus, giving a pI of 10 over the 54 first N-terminal residues, may explain the unexpected property of hPARP-3 to bind to and be moderately activated by DNA; however, up to now, no DNA has been detected in the centrosome.

The gene encoding hPARP-3 has been localized to the short arm of chromosome 3. Interestingly, allele loss involving the 3p arm is one of the most frequent and earliest known genetic events in lung cancer (Wistuba et al., 2000). Moreover, in the particular region 3p21.1 to 3p21.31 containing the *hPARP-3* gene a 600 kb region is most frequently undergoing allelic loss in the bronchial epithelia of smokers. It is therefore important to test whether hPARP-3 is present in lung epithelia, particularly in lung cancers.

PARP-3 localizes to the daughter centriole throughout the cell cycle

Indirect immunofluorescence experiments and subcellular fractionation concur to demonstrate that hPARP-3 is a core component of the centrosome. This particular localization, throughout the cell cycle, is independent of the microtubule polymerization status. Our data show that hPARP-3 is preferentially associated with the daughter centriole. Two independent lines of evidence support this idea: (i) in HeLa cells expressing GFP-centrin, PARP-3 immunostaining coincides with the smaller and less bright labelling already identified as the daughter centriole (White et al., 2000); and (ii) in mouse 3T3 cells, PARP-3 is clearly not associated with the primary cilium that identifies specifically the mature (mother) centriole during G1 phase (Chang and Stearns, 2000; Lange and Gull, 1995). Therefore, hPARP-3 appears to be the first known marker of the daughter centriole. What function does it exert here?

The mammalian centrosome is composed of two barrel-shaped centrioles, each formed by nine triplets of short microtubules, surrounded by a fibrous pericentriolar material. It is a vital organelle in animal cells as it directs the nucleation and organization of microtubules (Lange and Gull, 1996; Tassin and Bornens, 1999; Urbani and Stearns, 1999). As a consequence, the centrosome is essential during interphase for intracellular organelle transport, cell migration and the establishment of cell shape and polarity. The interphase centrosome then duplicates only once per cell cycle, thereby ensuring a strictly bipolar mitotic spindle axis (Mazia, 1984). Therefore, it plays a crucial role during mitosis in the equal and correct segregation of chromosomes as well as in the exit of cytokinesis (Piel et al., 2000). Indeed, many human tumor cells, including those lacking the tumor supressor p53 (Fukasawa et al., 1996), have abnormally high number of centrosomes (Pihan et al., 1998; Winey, 1996), and it has long been proposed that such aberrations may cause aneuploidy and contribute to cancer development (Brinkley, 2001; Doxsey, 1998). More recently, Nigg and collaborators (Meraldi et al., 2002; Meraldi and Nigg, 2001) have put forward a different mechanism where centrosome anomalies arise through failures in cell division, which lead to tetraploidization and subsequent propagation in tumor tissues, especially when the p53 pathway is abrogated or deregulated. Whatever the molecular scenario for the origin of centrosome aberrations may be, a strong correlation between centrosome amplification and aneuploidy exists and probably contributes to the selection of rare survival daughter cells that have acquired a mutator phenotype (Salisbury, 2001; Salisbury et al., 1999).

Overexpression of hPARP-3 or its N-terminal domain in HeLa cells interfered with the G1/S cell cycle transition, perhaps by titrating out a key regulator normally required at this critical stage when the decision to divide is taken. The lack of effect on HU-induced centrosome overduplication in CHO cells suggests that hPARP-3 does not interfere directly with

centrosome duplication. Our results rather point to a possible role for hPARP-3 in cell cycle progression at the G1/S transition. What is the connection between the influence of hPARP-3 at the G1/S transition and its preferential localization to the daughter centriole? The respective role of the two centrioles, mother and daughter, has been recently documented (Piel et al., 2000); they separate and function as independent structures at two stages of the cell division: (i) after the formation of the cleavage furrow, the mother centriole nucleates a microtubule aster, whereas the daughter centriole exhibits a considerable mobility, which progressively slows down from the onset of centrosome duplication at the G1/S border, up to late G2. (ii) At the end of telophase, just before abscission, the mother centriole moves to the intercellular bridge. Its repositioning back to the cell centre seems to provoke the completion of the cell division characterized by the narrowing of the intracellular bridge and abscission. On the basis of these observations, which clearly indicate that each centriole plays a specific role, it is tempting to speculate that hPARP-3, associated to the daughter centriole, may control its maturation until the G1/S restriction point is past. The regulating function of centrosome in the G1 to S transition has been recently studied using microsurgery and laser ablation. Indeed, when centrosomes were removed from somatic vertebrate cells, a proportion of cells completed cell division but failed to undergo the next round of DNA synthesis, suggesting a critical role of centrosomes in cell cycle progression (Hinchcliffe et al., 2001; Khodjakov and Rieder, 2001; Piel et al., 2000).

Alternatively, the presence of both hPARP-1 and hPARP-3 at the centrosome may be a part of a detection/signalling pathway aimed at monitoring the eventual presence, in the midbody, of broken DNA that originate from tension forces between two daughter cells experiencing unbalanced chromosome segregation. Indeed, both DNA and poly(ADP-ribose) can be easily detected in some arrested daughter cells as a long thin filament in the midbody (C.S. and G.dM., unpublished). Thus, DNA-binding enyzmes PARP-1 and PARP-3 might contribute to an ultimate cell division checkpoint linking the mitotic fidelity to the DNA damage surveillance network.

In conclusion, hPARP-3 and hPARP-1 add to the growing number of proteins that have been recently found, transiently or constitutively, associated with the centrosome. Conversely, the centrosomal protein centrin-2 has been recently identified as a constituent of the XPC (xeroderma pigmentosum) complex, a key component of global genome nucleotide excision repair acting as the initial damage detector (Araki et al., 2001), which points to an even more general link between DNA damage and repair and cell division (Su and Vidwans, 2000).

We are indebted to D. Muller for the reverse-transcribed RNA from lung tissue, to C. Celati for technical support, to B. Eddé for the Gt335 antibody, to J.-C. Amé and A.-M. Lambert for helpful discussions and to P. Chambon for constant support. This work was supported by funds from CNRS, Association pour la Recherche Contre le Cancer, Electricité de France, Ligue Nationale contre le Cancer, Commissariat à l'Energie Atomique and BASF AG. We acknowledge Incyte Pharmaceuticals for providing a partial human PARP-3 cDNA clone (#1889095) identified in the LifeSeqTM Database.

References

Amé, J. C., Rolli, V., Schreiber, V., Niedergang, C., Apiou, F., Decker, P., Muller, S., Hoger, T., Ménissier-de Murcia, J. and de Murcia, G. (1999). PARP-2, A novel mammalian DNA damage-dependent poly(ADP-ribose) polymerase. *J. Biol. Chem*. **274**, 17860-17868.

Apiou, F., Flagiello, D., Cillo, C., Malfoy, B., Poupon, M. F. and Dutrillaux, B. (1996). Fine mapping of human HOX gene clusters. *Cytogenet. Cell Genet*. **73**, 114-115.

Araki, M., Masutani, C., Takemura, M., Uchida, A., Sugasawa, K., Kondoh, J., Ohkuma, Y. and Hanaoka, F. (2001). Centrosome protein centrin 2/caltractin 1 is part of the xeroderma pigmentosum group C complex that initiates global genome nucleotide excision repair. *J. Biol. Chem*. **276**, 18665-18672.

Bailly, E., Doree, M., Nurse, P. and Bornens, M. (1989). p34cdc2 is located in both nucleus and cytoplasm; part is centrosomally associated at G2/M and enters vesicles at anaphase. *EMBO J*. **8**, 3985-3995.

Balczon, R., Bao, L., Zimmer, W. E., Brown, K., Zinkowski, R. P. and Brinkley, B. R. (1995). Dissociation of centrosome replication events from cycles of DNA synthesis and mitotic division in hydroxyurea-arrested Chinese hamster ovary cells. *J. Cell Biol*. **130**, 105-115.

Bornens, M. and Moudjou, M. (1999). Stuying the composition and function of centrosomes in vertebrates. *Methods Cell Biol.* **61**, 13-34.

Brinkley, B. R. (2001). Managing the centrosome numbers game: from chaos to stability in cancer cell division. *Trends Cell Biol*. **11**, 18-21.

Chang, P. and Stearns, T. (2000). Delta-tubulin and epsilon-tubulin: two new human centrosomal tubulins reveal new aspects of centrosome structure and function. *Nat. Cell Biol*. **2**, 30-35.

Chatton, B., Bahr, A., Acker, J. and Kedinger, C. (1995). Eukaryotic GST fusion vector for the study of protein protein associations in vivo: Application to interaction of ATFa with Jun and Fos. *Biotechniques* **18**, 142-145.

Cherney, B. W., McBride, O. W., Chen, D., Alkathib, H., Bhatia, K., Hensley, P. and Smulson, M. E. (1987). cDNA sequence, protein structure and chromosomal location of the human gene for poly(ADP-ribose) polymerase. *Proc. Natl. Acad. Sci. USA* **89**, 5789-5793.

Chi, N. W. and Lodish, H. F. (2000). tankyrase is a Golgi-associated MAP kinase substrate that interacts with IRAP in GLUT4 vesicles. *J. Biol. Chem.* **275**, 38437-38444.

Cook, B. D., Dynek, J. N., Chang, W., Shostak, G. and Smith, S. (2002). Role for the related poly(ADP-Ribose) polymerases tankyrase 1 and 2 at human telomeres. *Mol. Cell Biol*. **22**, 332-342.

D'Amours, D., Desnoyers, S., D'Silva, I. and Poirier, G. G. (1999). Poly(ADP-ribosyl)ation reactions in the regulation of nuclear functions. *Biochem. J*. **342**, 249-268.

de Murcia, G. and Ménissier de Murcia, J. (1994). Poly(ADP-ribose) polymerase: a molecular nick-sensor. *Trends Biochem. Sci*. **19**, 172-176.

de Murcia, G. and Shall, S. (2000). *From DNA Damage and Stress Signalling to Cell Death: Poly(ADP-ribosylation) Reactions.* Oxford: Oxford University Press.

Doxsey, S. (1998). The centrosome-a tiny organelle with big potential. *Nat. Genet*. **20**, 104-106.

Fukasawa, K., Choi, T., Kuriyama, R., Rulong, S. and Vande Woude, G. F. (1996). Abnormal centrosome amplification in the absence of p53. *Science* **271**, 1744-1747.

Giner, H., Simonin, F., de Murcia, G. and Ménissier-de Murcia, J. (1992). Overproduction and large-scale purification of the human poly(ADP-ribose) polymerase using a baculovirus expression system. *Gene* **114**, 279-283.

Hinchcliffe, E. H., Miller, F. J., Cham, M., Khodjakov, A. and Sluder, G. (2001). Requirement of a centrosomal activity for cell progression through G1 to S phase. *Science* **291**, 1499-1502.

Jacobson, M. K. and Jacobson, E. L. (1999). Discovering new ADP-ribose polymer cycles: protecting the genome and more. *Trends Biochem. Sci*. **24**, 415-417.

Johansson, M. (1999). A human poly(ADP-ribose) polymerase gene family (ADPRTL): cDNA cloning of two novel poly(ADP-ribose) polymerase homologues. *Genomics* **57**, 442-445.

Kanai, M., Uchida, M., Hanai, S., Uematsu, N., Uchida, K. and Miwa, M. (2000). Poly(ADP-ribose) localizes to the centrosomes and chromosomes. *Biochem. Biophys. Res. Commun.* **278**, 385-389.

Khodjakov, A. and Rieder, C. L. (2001). Centrosomes enhance the fidelity of cytokinesis in vertebrates and are required for cell cycle progression. *J. Cell Biol*. **153**, 237-242.

Kickhoefer, V. A., Siva, A. C., Kedersha, N. L., Inman, E. M., Ruland, C.,

Streuli, M. and Rome, L. H. (1999). The 193-kD vault protein, VPARP, is a novel poly(ADP-ribose) polymerase. *J. Cell Biol*. **146**, 917-928.

Kurosaki, T., Ushiro, H., Mitsuuchi, Y., Suzuki, S., Matsuda, M., Matsuda, Y., Katunuma, N., Kangawa, K., Matsuo, H., Hirose, T. et al. (1987). Primary structure of human poly(ADP-ribose) synthetase as deduced from cDNA sequence. *J. Biol. Chem*. **262**, 15990-15997.

Lange, B. M. and Gull, K. (1995). A molecular marker for centriole maturation in the mammalian cell cycle. *J. Cell Biol*. **130**, 919-927.

Lange, B. M. H. and Gull, K. (1996). Structure and function of the centriole in animal cells: progress and questions. *Trends Cell Biol.* **6**, 348-352.

Lemieux, N., Dutrillaux, B. and Viegas-Pequignot, E. (1992). A simple method for simultaneous R- or G-banding and fluorescence in situ hybridization of small single-copy genes. *Cytogenet. Cell Genet*. **59**, 311-312.

Lyons, R. J., Deane, R., Lynch, D. K., Jeffrey Ye, Z.-S., Sanderson, G. M., Eyre, H. J., Sutherland, G. R. and Daly, R. J. (2001). Identification of a novel human tankyrase through its interaction with the adaptor protein Grb14. *J. Biol. Chem.* **276**, 17172-17180.

Masson, M., Niedergang, C., Schreiber, V., Muller, S., Ménissier-de Murcia, J. and de Murcia, G. (1998). XRCC1 is specifically associated with poly(ADP-ribose) polymerase and negatively regulates its activity following DNA damage. *Mol. Cell Biol*. **18**, 3563-3571.

Matsumoto, Y., Hayashi, K. and Nishida, E. (1999). Cyclin-dependent kinase 2 (Cdk2) is required for centrosome duplication in mammalian cells. *Curr. Biol*. **9**, 429-432.

Mazen, A., Ménissier-de Murcia, J., Molinete, M., Simonin, F., Gradwohl, G., Poirier, G. and de Murcia, G. (1989). Poly(ADP-ribose)polymerase: a novel finger protein. *Nucleic Acids Res*. **17**, 4689-4698.

Mazia, D. (1984). Centrosomes and mitotic poles. *Exp. Cell Res*. **153**, 1-15.

Meraldi, P. and Nigg, E. A. (2001). Centrosome cohesion is regulated by a balance of kinase and phosphatase activities. *J. Cell Sci*. **114**, 3749-3757.

Meraldi, P., Lukas, J., Fry, A. M., Bartek, J. and Nigg, E. A. (1999). Centrosome duplication in mammalian somatic cells requires E2F and Cdk2-cyclin A. *Nat. Cell Biol*. **1**, 88-93.

Meraldi, P., Honda, R. and Nigg, E. A. (2002). Aurora-A overexpression reveals tetraploidization as a major route to centrosome amplification in p53–/– cells. *EMBO J*. **21**, 483-492.

Miranda, E. A., de Murcia, G. and Ménissier-de-Murcia, J. (1997). Large-scale production and purification of recombinant protein from an insect cell/baculovirus system in Erlenmeyer flasks: application to the chicken poly(ADP-ribose) polymerase catalytic domain. *Braz. J. Med. Biol. Res*. **30**, 923-928.

Moudjou, M. and Bornens, M. (1994). *Cell biology: a laboratory handbook*. New York: Academic Press, Inc.

Piel, M., Meyer, P., Khodjakov, A., Rieder, C. L. and Bornens, M. (2000). The respective contributions of the mother and daughter centrioles to centrosome activity and behavior in vertebrate cells. *J. Cell Biol*. **149**, 317-330.

Pihan, G. A., Purohit, A., Wallace, J., Knecht, H., Woda, B., Quesenberry, P. and Doxsey, S. J. (1998). Centrosome defects and genetic instability in malignant tumors. *Cancer Res*. **58**, 3974-3985.

Pockwinse, S. M., Krockmalnic, G., Doxsey, S. J., Nickerson, J., Lian, J. B., van Wijnen, A. J., Stein, J. L., Stein, G. S. and Penman, S. (1997). Cell cycle independent interaction of CDC2 with the centrosome, which is associated with the nuclear matrix-intermediate filament scaffold. *Proc. Natl. Acad. Sci. USA* **94**, 3022-3027.

Ruf, A., Ménissier de Murcia, J., de Murcia, G. and Schulz, G. E. (1996). Structure of the catalytic fragment of poly(AD-ribose) polymerase from chicken. *Proc. Natl. Acad. Sci. USA* **93**, 7481-7485.

Salisbury, J. L. (2001). The contribution of epigenetic changes to abnormal centrosomes and genomic instability in breast cancer. *J. Mammary Gland Biol. Neoplasia* **6**, 203-212.

Salisbury, J. L., Whitehead, C. M., Lingle, W. L. and Barrett, S. L. (1999). Centrosomes and cancer. *Biol. Cell* **91**, 451-460.

Sato, N., Mizumoto, K., Nakamura, M. and Tanaka, M. (2000). Radiation-induced centrosome overduplication and multiple mitotic spindles in human tumor cells. *Exp. Cell Res*. **255**, 321-326.

Sbodio, J. I., Lodish, H. F. and Chi, N. W. (2002). Tankyrase-2 oligomerizes with tankyrase-1 and binds to both TRF1 (telomere-repeat-binding factor 1) and IRAP (insulin-responsive aminopeptidase). *Biochem. J*. **361**, 451-459.

Schreiber, V., Ame, J. C., Dolle, P., Schultz, I., Rinaldi, B., Fraulob, V., Ménissier-de Murcia, J. and de Murcia, G. (2002). Poly(ADP-ribose) polymerase-2 (PARP-2) is required for efficient base excision DNA repair in association with PARP-1 and XRCC1. *J Biol. Chem*. **277**, 23028-23036.

Shall, S. and de Murcia, G. (2000). Poly(ADP-ribose) polymerase-1: what have we learned from the deficient mouse model? *Mutat. Res*. **460**, 1-15.

Smith, S. (2001). The world according to PARP. *Trends Biochem. Sci.* **26**, 174-179.

Smith, S. and de Lange, T. (1999). Cell cycle dependent localization of the telomeric PARP, tankyrase, to nuclear pore complexes and centrosomes. *J. Cell Sci*. **112**, 3649-3656.

Smith, S. and de Lange, T. (2000). Tankyrase promotes telomere elongation in human cells. *Curr. Biol*. **10**, 1299-1302.

Smith, S., Giriat, I., Schmitt, A. and de Lange, T. (1998b). Tankyrase, a poly(ADP-ribose) polymerase at human telomeres. *Science* **282**, 1484-1487.

Su, T. T. and Vidwans, S. J. (2000). DNA defects target the centrosome [news; comment]. *Nat. Cell Biol*. **2**, E28-E29.

Tassin, A. M. and Bornens, M. (1999). Centrosome structure and microtubule nucleation in animal cells. *Biol. Cell* **91**, 343-354.

Uchida, K., Morita, T., Sato, T., Ogura, T., Yamashita, R., Nogushi, S., Suzuki, H., Nyunoya, H., Miwa, M. and Sugimura, T. (1987). Nucleotide sequence of a full length cDNA for human fibroblast poly(ADP-ribose)polymerase. *Biochem. Biophys. Res. Commun.* **148**, 617-622.

Urbani, L. and Stearns, T. (1999). The centrosome. *Curr. Biol*. **9**, R315-R317.

White, R. A., Pan, Z. and Salisbury, J. L. (2000). GFP-centrin as a marker for centriole dynamics in living cells. *Microsc. Res. Tech*. **49**, 451-457.

Winey, M. (1996). Keeping the centrosome cycle on track. Genome stability. *Curr. Biol.* **6**, 962-964.

Wistuba, I. I., Behrens, C., Virmani, A. K., Mele, G., Milchgrub, S., Girard, L., Fondon, J. W., 3rd, Garner, H. R., McKay, B., Latif, F., Lerman, M. I., Lam, S., Gazdar, A. F. and Minna, J. D. (2000). High resolution chromosome 3p allelotyping of human lung cancer and preneoplastic/preinvasive bronchial epithelium reveals multiple, discontinuous sites of 3p allele loss and three regions of frequent breakpoints. *Cancer Res*. **60**, 1949-1960.